J|A|C|S
ARTICLES
Published on Web 01/04/2008

NMR Investigations of the Static and Dynamic Structures of Bisphosphonates on Human Bone: a Molecular Model

Sujoy Mukherjee,† Yongcheng Song,‡ and Eric Oldfield*,†,‡

Center for Biophysics and Computational Biology, 607 South Mathews Avenue, University of Illinois at Urbana-Champaign, Urbana, Illinois 61801, Department of Chemistry, University of Illinois at Urbana-Champaign, 600 South Mathews Avenue, Urbana, Illinois 61801

Received August 9, 2007; E-mail: eo@chad.scs.uiuc.edu

Abstract: We report the results of an investigation of the binding of a series of bisphosphonate drugs to human bone using ^{2}H, ^{13}C, ^{15}N, and ^{31}P nuclear magnetic resonance spectroscopy. The ^{31}P NMR results show that the bisphosphonate groups bind irrotationally to bone, displacing orthophosphate from the bone mineral matrix. Binding of pamidronate is well described by a Langmuir-like isotherm, from which we deduce an ~30−38 Å^2 surface area per pamidronate molecule and a $\Delta G = -4.3$ kcal mol^{-1}. TEDOR of [$^{13}C_3$, ^{15}N] pamidronate on bone shows that the bisphosphonate binds in a gauche [N−C(1)] conformation. The results of ^{31}P as well as ^{15}N shift and cross-polarization measurements indicate that risedronate binds weakly, since it has a primarily neutral pyridine side chain, whereas zoledronate (with an imidazole ring) binds more strongly, since the ring is partially protonated. The results of ^{2}H NMR measurements of side-chain ^{2}H-labeled pamidronate, alendronate, zoledronate, and risedronate on bone show that all side chains undergo fast but restricted motions. In pamidronate, the motion is well simulated by a *gauche*$^+$/*gauche*$^-$ hopping motion of the terminal $-CH_2-NH_3^+$ group, due to jumps from one anionic surface group to another. The results of double-cross polarization experiments indicate that the NH_3^+-terminus of pamidronate is close to the bone mineral surface, and a detailed model is proposed in which the *gauche* side-chain hops between two bone PO_4^{3-} sites.

1. Introduction

Bisphosphonate drugs such as pamidronate (**1**, Aredia), risedronate (**2**, Actonel), zoledronate (**3**, Zometa) and alendronate (**4**, Fosamax) are used to treat a variety of bone resorption diseases, such as osteoporosis, Paget's disease, and hypercalcemia due to malignancy.[1] They are thought to act by inhibiting the enzyme farnesyl diphosphate synthase,[2] resulting in inhibition of protein prenylation in osteoclasts. In addition to their use in treating these diseases, bisphosphonates have also been found[3] to activate $\gamma\delta$ T cells (containing the Vγ2Vδ2 T cell receptor) of the immune system, which then kill tumor cells;[4] plus, they have direct activity against tumor cell growth,[5] as well as the growth of a variety of pathogenic protozoa[6] and some bacteria.[7] There is thus interest in studying in more detail how bisphosphonates bind to human bone, since this could have important implications for their future development in oncology and as anti-infectives, where, in general, bone binding might be expected to reduce efficacy.

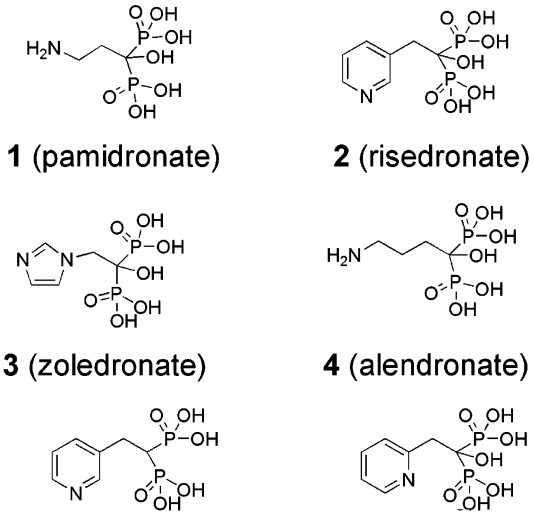

In recent work, several groups have used chromatographic and other methods to investigate how bisphosphonates bind to hydroxyapatite,[8−10] one component of bone mineral. However, because bone contains ~25−40% protein[11] (mainly collagen)

† Center for Biophysics and Computational Biology.
‡ Department of Chemistry.

(1) Russell, R. G. *Ann. N. Y. Acad. Sci.* **2006**, *1068*, 367−401.
(2) Rondeau, J. M.; Bitsch, F.; Bourgier, E.; Geiser, M.; Hemmig, R.; Kroemer, M.; Lehmann, S.; Ramage, P.; Rieffel, S.; Strauss, A.; Green, J. R.; Jahnke, W. *ChemMedChem.* **2006**, *1*, 267−273.
(3) Kunzmann, V.; Bauer, E.; Wilhelm, M. *N. Engl. J. Med.* **1999**, *340*, 737−738.
(4) Wilhelm, M.; Kunzmann, V.; Eckstein, S.; Reimer, P.; Weissinger, F.; Ruediger, T.; Tony, H. P. *Blood* **2003**, *102*, 200−206.
(5) Kunzmann, V.; Bauer, E.; Feurle, J.; Weissinger, F.; Tony, H. P.; Wilhelm, M. *Blood* **2000**, *96*, 384−392.
(6) Martin, M. B.; Grimley, J. S.; Lewis, J. C.; Heath, H. T., 3rd; Bailey, B. N.; Kendrick, H.; Yardley, V.; Caldera, A.; Lira, R.; Urbina, J. A.; Moreno, S. N.; Docampo, R.; Croft, S. L.; Oldfield, E. *J. Med. Chem.* **2001**, *44*, 909−916.
(7) Leon, A.; Liu, L.; Yang, Y.; Hudock, M. P.; Hall, P.; Yin, F.; Studer, D.; Puan, K. J.; Morita, C. T.; Oldfield, E. *J. Med. Chem.* **2006**, *49*, 7331−7341.

10.1021/ja0759949 CCC: $40.75

and because there are only relatively low levels of hydroxyapatite present in the mineral phase[12,13] (the major component is carbonatoapatite), it is clearly of interest to probe in a more direct fashion how bisphosphonates bind to human bone. Moreover, chromatographic methods give no direct information on either the static or the dynamic structures of bound bisphosphonates, or information on their protonation states. It is likewise unclear whether binding is primarily a physisorption process, or involves displacement of phosphate groups by the anionic bisphosphonate ligands. Here, we thus report the results of a series of liquid- and solid-state NMR investigations of the interactions between bisphosphonates and human bone. Solid-state NMR is an ideal technique with which to investigate the structures (static and dynamic) of molecules bound to bone surfaces, and has previously been used to investigate the structures of bone mineral,[12,13] as well as of a bone-seeking peptide, statherin, interacting with hydroxyapatite.[14] We show that bisphosphonates bind tightly to human bone (displacing PO_4^{3-}); that their sidechains exhibit restricted mobility; that protonation states can be observed directly, and that, in the case of pamidronate, the bound drug conformation can be determined experimentally, leading to a detailed molecular model for pamidronate-bone binding.

2. Materials and Methods

2.1. NMR Spectroscopy. Solid-state NMR spectra were obtained by using the magic-angle sample spinning technique using 600 MHz (^{1}H resonance frequency) Infinity Plus spectrometers (Varian, Palo Alto, CA) equipped with 14.1 T, 2.0 and 3.5 in. bore Oxford magnets and Varian/Chemagnetics 3.2 and 4.0 mm T3 HXY probes. For ^{13}C and ^{15}N NMR experiments, spectra were obtained by using cross-polarization and with TPPM[15] decoupling. Proton decoupled solid-state ^{31}P spectra were recorded with and without (for quantitation) cross polarization, while liquid-state spectra were acquired with full proton decoupling. For pamidronate, a two-dimensional ^{13}C−^{13}C correlation spectrum was obtained by using radio frequency driven recoupling (RFDR).[16] A heteronuclear, broadband double cross polarization[17] (DCP) experiment[18] was performed for ^{13}C−^{31}P chemical shift correlation of pamidronate on bone and TEDOR[19] was used for N−C distance determinations, on the same sample. All ^{13}C, ^{15}N, and ^{31}P spectra were obtained at ∼30 °C, with the exception of the TEDOR and DCP spectra, which were obtained at 0 °C (to provide a slight enhancement in sensitivity and minimize the probability of water loss during the long data acquisition period). All 2D NMR experiments were processed with NMRPipe[20] and Sparky[21] was used for visualization and analysis. For ^{2}H NMR, a solid echo pulse sequence ($90_{\pm x} - t - 90_y -$) was used and the signal was left shifted to the echo maximum prior to data processing.[22] ^{13}C NMR chemical shifts were referenced with respect to the downfield peak of adamantane (taken to be 38.48 ppm from TMS); ^{15}N shifts are reported with respect to a liquid NH_3 standard taking an external reference of 1 M $^{15}N_2$-urea in DMSO to be at 79.4 ppm downfield from NH_3,[23] and ^{31}P NMR chemical shifts were referenced with respect to an external standard of 85% orthophosphoric acid. All shifts use the IUPAC convention that high frequency, paramagnetic, downfield or deshielded values are positive. Deuterium line shape simulations were carried out by using the Turbopowder program.[24]

2.2. Synthesis of ^{2}H, ^{13}C, and ^{15}N-Labeled Bisphosphonates. 2.2.1. General Procedure: A mixture of a carboxylic acid (1 mmol), H_3PO_3 (5 mmol) and toluene (4 mL) was heated to 80 °C with stirring. After all solids melted, $POCl_3$ (5 mmol) was added slowly and the mixture stirred vigorously at 80 °C for 5 h.[25] Upon cooling, the toluene was decanted, and 6 N HCl (3 mL) was added to the residue. The resulting solution was stirred for 6 h, after which most of the solvent was removed *in vacuo*. Isopropanol (25 mL) was added to precipitate a 1-hydroxymethylene bisphosphonate as a white powder, which was filtered, washed with ethanol (5 × 5 mL), dried, and then further purified by recrystallization from H_2O/EtOH. All compounds had satisfactory C, H, N microanalyses and ^{1}H solution NMR spectra.

2.2.1.1. 1-Hydroxy-3-aminopropyl-1,1-bisphosphonic Acid-$^{13}C_3$, ^{15}N (Pamidronic Acid-$^{13}C_3$, ^{15}N). This compound was made from [$^{13}C_3$, ^{15}N] β-alanine (Cambridge) (250 mg), following the above general procedure (205 mg, 45%).

2.2.1.2. 1-Hydroxy-3-aminopropyl-1,1-bisphosphonic Acid-2,2,3,3,-$^2H_4$ (Pamidronic Acid-d_4). This compound was made from β-alanine-2,2,3,3-$^2H_4$ (C/D/N Isotopes, Quebec, Canada) (250 mg), following the above general procedure (225 mg, 50%)

2.2.1.3. 1-Hydroxy-4-aminobutyl-1,1-bisphosphonic Acid-2,2,3,3,4,4-$^2H_6$ (Alendronic Acid-d_6). This compound was made from [2,2,3,3,4,4-$^2H_6$]-4-aminobutyric acid (Aldrich) (250 mg), following the above general procedure (210 mg, 47%).

2.2.1.4. 1-Hydroxy-2-($^{15}N_2$]-imidazol-1-yl)-1,1-bisphosphonic Acid ($^{15}N_2$-zoledronic Acid). This compound was made from [$^{15}N_2$]-imidazole-1-acetic acid, which was prepared according to a published procedure[25,26] from [$^{15}N_2$]-imidazole (Cambridge) (260 mg), following the above general procedure (265 mg, 26%).

2.2.1.5. 1-Hydroxy-2-([2,4,5,6-$^2H_4$]-pyridin-3-yl)ethylidene-1,1-bisphosphonic Acid- (Risedronic Acid-d_4). [2,4,5,6-$^2H_4$]-3-Pyridinylacetic acid-was prepared according to a published procedure[27] from [2,4,5,6-$^2H_4$]-3-bromopyridine,[28] followed by hydrolysis (1 N DCl, reflux). [2,4,5,6-$^2H_4$]-risedronic acid was made from the acid obtained (137 mg) following the above general procedure (185 mg, 65%).

2.2.2. Preparation of Bisphosphonate-Bone Samples. Human bone tissue (non-demineralized bone powder, gun-shot victim, 45−125μm particle size,) was obtained from the Pacific Coast Tissue Bank (Los Angeles, CA) and was used without further treatment. Typically, 50

(8) Lawson, M. A.; Triffitt, J. T.; Ebetino, F. H.; Barnett, B. L.; Phipps, R. J.; Locklin, R. M.; Russell, R. G. G. *J. Bone Min. Res.* **2005**, *20*, S396.
(9) Nancollas, G. H.; Tang, R.; Phipps, R. J.; Henneman, Z.; Gulde, S.; Wu, W.; Mangood, A.; Russell, R. G.; Ebetino, F. H. *Bone* **2006**, *38*, 617−627.
(10) Robinson, J.; Cukrowski, I.; Marques, H. M. *J. Mol. Struct.* **2006**, *825*, 134−142.
(11) Aerssens, J.; Boonen, S.; Lowet, G.; Dequeker, J. *Endocrinology* **1998**, *139*, 663−670.
(12) Cho, G. Y.; Wu, Y. T.; Ackerman, J. L. *Science* **2003**, *300*, 1123−1127.
(13) Kolodziejski, W. New Techniques in Solid-State NMR. *Top. Curr. Chem.* **2005**, *246*, 235−270.
(14) Goobes, G.; Goobes, R.; Schueler-Furman, O.; Baker, D.; Stayton, P. S.; Drobny, G. P. *Proc. Natl. Acad. Sci. U.S.A.* **2006**, *103*, 16083−16088.
(15) Bennett, A. E.; Rienstra, C. M.; Auger, M.; Lakshmi, K. V.; Griffin, R. G. *J. Chem. Phys.* **1995**, *103*, 6951−6958.
(16) Bennett, A. E.; Ok, J. H.; Griffin, R. G.; Vega, S. *J. Chem. Phys.* **1992**, *96*, 8624−8627.
(17) Hediger, S.; Meier, B. H.; Ernst, R. R. *Chem. Phys. Lett.* **1995**, *240*, 449−456.
(18) Schaefer, J.; Mckay, R. A.; Stejskal, E. O. *J. Magn. Reson.* **1979**, *34*, 443−447.
(19) Jaroniec, C. P.; Filip, C.; Griffin, R. G. *J. Am. Chem. Soc.* **2002**, *124*, 10728−10742.
(20) Delaglio, F.; Grzesiek, S.; Vuister, G. W.; Zhu, G.; Pfeifer, J.; Bax, A. *J. Biomol. NMR* **1995**, *6*, 277−293.
(21) Goddard, T. D.; Kneller, D. G. University of California, San Francisco. http://www.cgl.ucsf.edu/home/sparky/.
(22) Davis, J. H.; K. R. J.; Bloom, M.; Valic, M. I.; Higgs, T. P. *Chem. Phys. Lett.* **1976**, *42*.
(23) Wishart, D. S.; Bigam, C. G.; Yao, J.; Abildgaard, F.; Dyson, H. J.; Oldfield, E.; Markley, J. L.; Sykes, B. D. *J. Biomol. NMR* **1995**, *6*, 135−140.
(24) Wittebort, R. J.; Olejniczak, E. T.; Griffin, R. G. *J. Chem. Phys.* **1987**, *86*, 5411−5420.
(25) Harel, Z.; Kovalevski-Liron, E.; Lidor-Hadas, R.; Lifshitz-Liron, R. Use of certain diluents for making bisphosphonic acids. World Patent WO03097655. November 27, 2003.
(26) Gil, M. S.; Cruz, F.; Cerdan, S.; Ballesteros, P. *Bioorg. Med. Chem. Lett.* **1992**, *2*, 1717−1722.
(27) Kondo, Y.; Inamoto, K.; Uchiyama, M.; Sakamoto, T. *Chem. Commun.* **2001**, 2704−2705.
(28) Sirimanne, S. R.; Maggio, V. L.; Patterson, D. G. *J. Lab. Comp. & Radiopharm.* **1992**, *31*, 163−174.

mg of bone powder was suspended in 1 mL H_2O and the bisphosphonate was dissolved in 1 mL of H_2O. The pH of both samples was adjusted to the pH of interest, and the samples were then mixed, and the pH adjusted (with concentrated NaOH or HCl) as needed. Samples were incubated for 1 h and centrifuged, after which the supernatant was removed. The bone-bisphosphonate pellets were then washed with 2 mL of Millipore water and packed into NMR rotors. In some cases, the supernatant solutions were also investigated by solution NMR using an external NaH_2PO_4 quantitation standard (doped with 10 μM $FeCl_3$).

3. Results and Discussion

3.1. Chemisorption of Bisphosphonates to Bone. In Figure 1A−D, we show the ^{31}P MAS NMR spectra of three different bisphosphonates: zoledronate (**3**), pamidronate (**1**), and deoxy-risedronate (**5**), bound to human bone at pH = 7 together with, inset, the ^{31}P MAS NMR spectra of the pure bisphosphonates. In each case, the bone spectra consist of two sets of resonances (and their associated side-bands): a sharp feature at ~3 ppm corresponding to orthophosphate in the bone mineral, and a second, broader and weaker feature at ~15 ppm, due to the bisphosphonate bound to bone. The bisphosphonate peak is featureless, unlike those seen in the spectra of the corresponding crystalline bisphosphonates, and has essentially the same width and shift at 10^5, 10^4, and 10^3 ppm loadings, disappearing into the noise level at ~100 ppm (Figures 2A−D) No other peaks were observed. These observations are similar to those made by Josse et al.,[29] who found that zoledronate (**3**) bound to a variety of calcium phosphate compounds (β-tricalcium phosphate; calcium-deficient apatites), of interest as novel biomaterials for drug delivery, with a relatively broad, featureless line shape.[29] The lack of any discernible structure would, however, be consistent with either physisorption or chemisorption. That is, the bisphosphonates might undergo either relatively weak electrostatic interactions with the inorganic components of bone, together with hydrophobic interactions with the collagen component, or they might be involved in the displacement of anionic groups (OH^-, CO_3^{2-}, and PO_4^{3-}), with the bisphosphonate PO_3 groups substituting for these anions in the lattice. And, of course, both types of interaction might occur. The "chemical" displacement interaction might be expected to be more likely, because bisphosphonates are known to have half-lives in bone on the order of many years; plus, this displacement mechanism would give at least a qualitative explanation of the observation that high levels of PO_4^{3-} are required to elute bisphosphonates from hydroxyapatite in chromatographic adsorption experiments.[8] The NMR results support several aspects of this strong chemisorption model. First, the overall spans of the chemical shielding tensors are ~120 ppm, similar to those seen in crystalline bisphosphonates,[30] indicating no significant motional averaging of the chemical shift anisotropy. If only physisorption were involved, then considerable narrowing the ^{31}P spectral width would seem likely, due to fast motion on the bone surface. Second, an analysis of the supernatants in our experiments by solution ^{31}P NMR shows that there is, in fact, release of inorganic phosphate on bisphosphonate addition with, on average, ~1.25 bisphosphonates binding per phosphate released, essentially the same effect as that seen with the synthetic calcium phosphate compounds investigated by Josse et al.[29] So, bisphosphonates bind in an irrotational manner to bone (or, at least, these are no fast, large-angle motions of the bisphosphonate backbone), and this can be attributed, at least in part, to displacement of inorganic phosphate by at least one phosphonate group, enabling strong bisphosphonate interactions with Ca^{2+} in the bone mineral matrix.

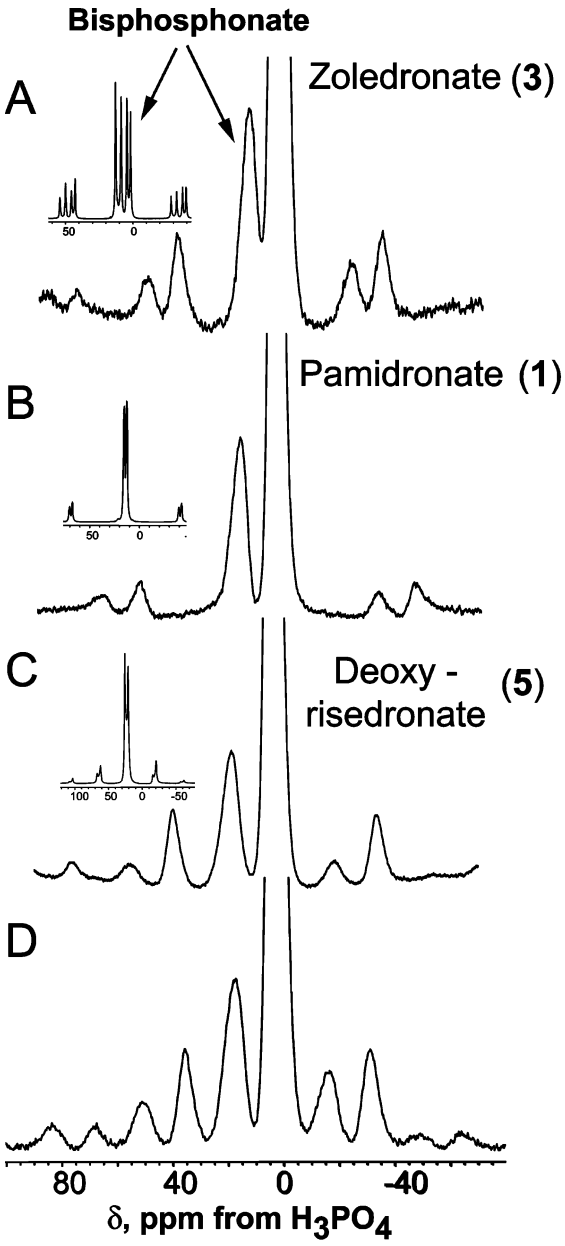

Figure 1. ^{31}P MAS NMR spectra (600 MHz ^{1}H resonance frequency) of bisphosphonates bound to bone (A−D) together with (inset), spectra of the corresponding crystalline bisphosphonates. All spectra were obtained by using cross-polarization followed by TPPM decoupling during data acquisition. (A) zoledronate on bone, 2 s recycle, 8192 scans and 10 kHz spin speed; (B) pamidronate on bone, 5 s recycle, 1024 scans and 13.333 kHz spin speed; (C) deoxy-risedronate on bone, 2 s recycle, 16384 scans and 10 kHz spin speed; and (D) pamidronate on bone, 2 s recycle, 4096 scans and 8 kHz spin speed. All FIDs were processed with 50 Hz line broadening.

Interestingly, the area of the bisphosphonate surface peak observed does not correlate in a linear way with the amount of bisphosphonate added to the sample. Rather, our results indicate that binding exhibits the type of sigmoid binding behavior seen with chemisorption, as expected for example by the Langmuir-

(29) Josse, S.; Faucheux, C.; Soueidan, A.; Grimandi, G.; Massiot, D.; Alonso, B.; Janvier, P.; Laib, S.; Pilet, P.; Gauthier, O.; Daculsi, G.; Guicheux, J. J.; Bujoli, B.; Bouler, J. M. *Biomaterials* **2005**, *26*, 2073−80.
(30) Zhang, Y.; Oldfield, E. *J. Phys. Chem. B* **2006**, *110*, 579−586.

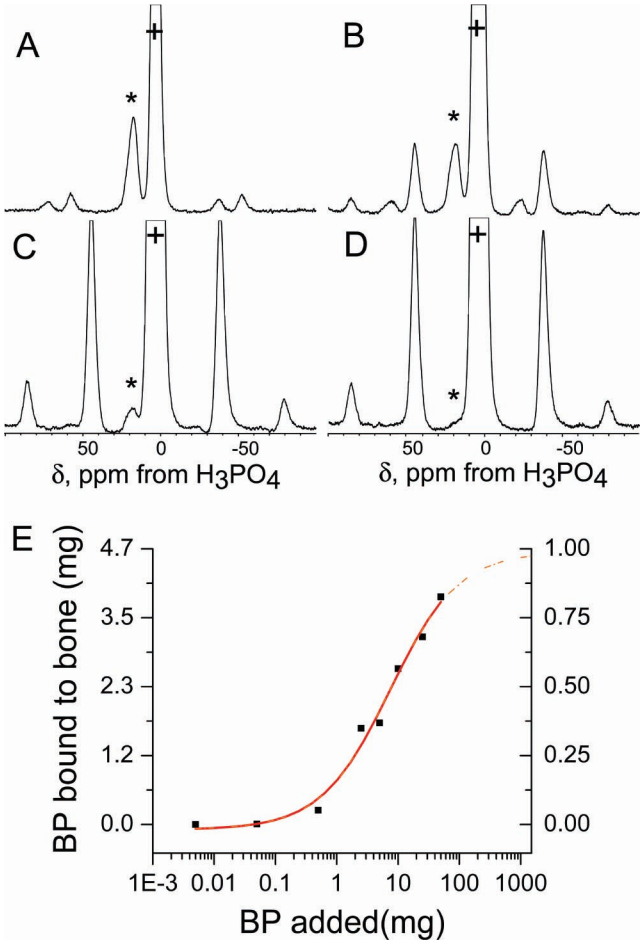

Figure 2. ^{31}P MAS NMR spectra of pamidronate on bone and Langmuir adsorption isotherm. (A), 3×10^5 ppm pamidronate solution used in sample preparation; (B) 10^4 ppm solution concentration; (C) 10^3 ppm; (D), 10^2 ppm + = bone mineral PO_4^{3-} peak, * = bisphosphonate peak. (E), Langmuir adsorption isotherm. Y-axis at left indicates mg pamidronate bound, *y*-axis at right indicates θ ($\theta = 1$ for monolayer coverage).

like binding isotherm for the reaction:

$$\mathrm{BP(solution)} + \mathrm{S} \underset{k_{-1}}{\overset{k_1}{\rightleftharpoons}} \mathrm{BP{\bullet}S\ (bound)}$$

where BP = bisphosphonate, S = bone surface, and the surface coverage, θ, is given by the following:

$$\theta = K[c]/(1+K[c])$$

where $[c]$ is the concentration of bisphosphonate in solution and $K = k_1/k_{-1}$. At low $[c]$, $\theta \propto [c]$, whereas in the limit [c] $\rightarrow \infty$, θ=1. The binding of the salivary protein statherin to HAP has also been shown to follow Langmuir-binding behavior,[31] from which information on the thermodynamics of binding can be deduced. We thus obtained ^{31}P MAS NMR spectra of pamidronate bound to bone at eight concentrations (representative spectra are shown in Figures 2A−D), then plotted the relative bisphosphonate: bone area versus the amount of BP (pamidronate) used and fitted the data to a rectangular hyperbolic function, Figure 2E [the Y axes are bound pamidronate (left) and θ (right), respectively]. The graph can be calibrated by using our observation that the addition of 2.7 mg pamidronate results in 1.41 mg of bisphosphonate being bound per 50 mg bone sample, from which we deduce that the maximum coverage corresponds to 4.68 mg of bound pamidronate. Given that the mineral component of human bone has a surface area area of ~110 m^2/gram[32,33] and that ~60−75% of bone is composed of this mineral component,[11] we can deduce a surface area of pamidronate on bone as: (bone mineral surface area in sample)/(number of pamidronate molecules bound) = (110 m^2/g × 0.05 g × (0.6−0.75) × 10^{20} Å^2)/ (6.023 × 10^{23} × 0.00468 g/270 g/mol (Na^+pamidronate·H_2O Fwt)) ~30−38 Å^2/ molecule. This value is close to that the 40 Å^2/molecule that can be deduced from the unit cell dimensions of monosodium pamidronate,[34] and indicates that pamidronate molecules are quite highly packed on the mineral component of human bone, at high coverage, although as shown in Figure 1B, the ^{31}P MAS NMR spectra of crystalline pamidronate are of course quite different. From the isotherm, we obtain $\Delta G = -4.3$ kcal mol^{-1} for pamidronate binding to human bone mineral.

This type of chemisorption is only seen at pH = 7, and without any pH control, we find that a separate bisphosphonate phase can form. For example, addition of the free zwitterionic risedronic acid to bone (in H_2O) results in the appearance of new resonances at δ = 15.0, 16.1 ppm, the same as seen in a sample of Ca^{2+}-risedronate prepared by adding $Ca(NO_3)_2$ to risedronate at low pH. X-ray powder diffraction of such samples at high bisphosphonate loading reveals sharp diffraction peaks that are the same as those found in Ca^{2+}-risedronate, indicating formation of a new nanocrystalline phase, due to displacement of bone Ca^{2+}. This result is similar to that observed by Josse et al.[29] on zoledronate addition to a calcium phosphate phase, but seems unlikely to be of physiological relevance. So, the results of Figure 2 support the idea that, at pH ≈ 7, bisphosphonate chemisorbs to human bone mineral surface, forming, at high concentrations, a monolayer.

In addition to displacing P_i and interacting with Ca^{2+}, there is also now evidence for the importance of the 1-OH group on the bisphosphonate backbone in binding to hydroxyapatite,[8] as well as the importance of side chain charge and location.[8] This is evidenced by differences in the affinity for hydroxyapatite in chromatographic experiments by, e.g., zoledronate and risedronate,[8] whose side chains have different pK_a values, as well as by ^{31}P NMR results, on bone. At pH = 4.0, the pyridine ring in risedronate is protonated, since the pK_a value of the pyridine ring is ~5.7, and this protonation enables the ready cross-polarization of [^{15}N]-risedronate bound to bone, as shown in Figure 3A. The ^{31}P MAS NMR spectrum also indicates strong bone binding, as seen in Figure 3B. At pH = 6.0, however, the ^{15}N NMR cross polarization peak intensity is much weaker (about the same as the intensity arising from the ^{15}N-sites in collagen[35]), Figure 3C, although the ^{31}P peak from the chemisorbed bisphosphonate is still pronounced (Figure 3D). This is consistent with a decrease in bone adsorption due to the fact that the pyridine ring nitrogen is now (on average) far less protonated than that at pH = 4.0. At pH = 8.0, the pyridinium ^{15}N peak is no longer detectable (Figure 3E) although the surface

(31) Goobes, R.; Goobes, G.; Shaw, W. J.; Drobny, G. P.; Campbell, C. T.; Stayton, P. S. *Biochemistry* **2007**, *46*, 4725−4733.
(32) Holmes, J. M.; Davies, D. H.; Meath, W. J.; Beebe, R. A. *Biochemistry* **1964**, *3*, 2019−2024.
(33) Kolmas, J.; Slosarczyk, A.; Wojtowicz, A.; Kolodziejski, W. *Solid State Nucl. Magn. Reson.* **2007**, *32*, 53−58.
(34) Stahl, K.; Treppendahl, S. P.; Preikschat, H.; Fischer, E. *Acta Cryst. Section E-Struct. Reports Online* **2005**, *61*, M132−M134.
(35) Naito, A.; Tuzi, S.; Saito, H. *Eur. J. Biochem.* **1994**, *224*, 729−734.

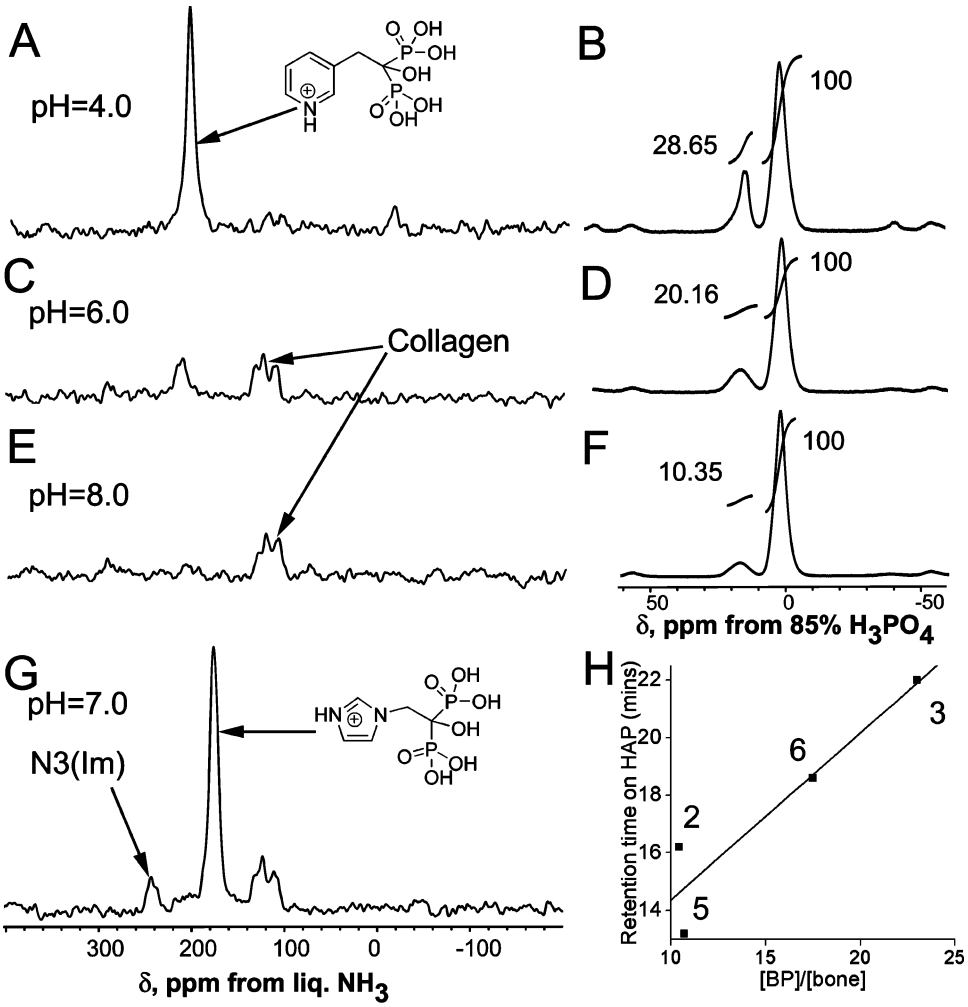

Figure 3. ^{15}N and ^{31}P MAS NMR of bisphosphonates on bone. (A−F), ^{15}N (A, C, E) and ^{31}P (B, D, F) MAS NMR spectra of [^{15}N]-risedronate on bone at the pH values indicated. (G) ^{15}N MAS NMR spectrum of [$^{15}N_2$]-zoledronate on bone, pH = 7.0. The natural abundance level ^{15}N signals from collagen are indicated. At pH = 7.0, there is a small resonance from N3 of the neutral imidazole side chain, at 245 ppm. Spectra were typically obtained by using a 3.38 μs 90° pulse, a mix pulse of 6 ms (^{15}N NMR) or 1 ms (for ^{31}P NMR), followed by data acquisition for 1024 points with a dwell time of 20 μs. A pulse delay of 3 s (for ^{15}N) or 2 s (for ^{31}P) was used. FIDs were zero-filled to 2048 points and processed with 200 Hz (^{15}N NMR) or 50 Hz (^{31}P NMR) line-broadening prior to Fourier transformation. All ^{31}P NMR spectra were obtained with 8192 scans, while the ^{15}N spectra required from 65536 to 100 000 scans. (H) Comparison plot of retention times of bisphosphonates (zoledronate (**3**), ortho-risedronate (**6**), risedronate (**2**) and deoxy-risedronate (**5**) on HAP obtained by column chromatography[8] versus the ratio of the bisphosphonate/ bone ^{31}P peak areas; $R^2 = 0.88$.

bisphosphonate peak is still observable (Figure 3F) but is clearly less intense than that at the lower pH values. Clearly, these ^{15}N and ^{31}P NMR results indicate that side-chain deprotonation is associated with weaker bone binding. In the case of [$^{15}N_2$]-zoledronate bound to bone at pH = 7.0, the ^{15}N MAS NMR spectrum (Figure 3G) is more intense than that seen with risedronate at either pH = 6 or 8, consistent with the fact that the imidazole side chain of zoledronate is expected to have a $pK_a \approx 6.7$ and is, therefore, more highly protonated, resulting in increased cross polarization as well as enhanced electrostatic interactions with anionic groups on the bone surface. On the basis of integrated ^{31}P CP-MAS NMR peak areas, we find that pamidronate and zoledronate bind most strongly to human bone (28.7, 23% bisphosphonate: bone peak areas), followed by *ortho*-risedronate (**6**) and alendronate (17.5, 16.9%), with weaker binding of risedronate and deoxy-risedronate (10.4, 10.7%). For the four compounds (**2**, **3**, **5**, **6**) where chromatographic retention times on HAP are available,[8] these results correlate quite well ($R^2 = 0.88$, Figure 3H) with the HAP retention times, suggesting that binding to the collagen component in bone is not significant, at least for these bisphosphonates. Although the protonation state of bound bisphosphonates might of course be guessed from pK_a values alone, this approach clearly does not work with bisphosphonates bound to their target FPPS enzyme, where both risedronate and zoledronate bind in a fully protonated state[36] (at pH = 7.0), even though there are no obvious nearby proton sources present in the active site, warranting therefore these ^{15}N NMR experiments on bone. But what are the structures—static and dynamic, of these adsorbed bisphosphonates?

3.2. Static and Dynamic Structures of Bound Bisphosphonates. We thus next investigated the structures (static and/or dynamic) of several bisphosphonates bound to bone. We elected to begin by investigating the static and dynamic structure of pamidronate (**1**, Aredia), since this is the simplest nitrogen-containing bisphosphonate drug and can be readily prepared as the [^{13}C, ^{15}N]-labeled isotopomer from commercially available [$^{13}C_3$, ^{15}N] β-alanine. The 1D ^{13}C CP-MAS NMR spectrum of [$^{13}C_3$, ^{15}N]-pamidronate is shown in Figure 4A, and consists of the resonance of C_1 (J-coupled to P_1 and P_2) at 73 ppm, with

(36) Mao, J. H.; Mukherjee, S.; Zhang, Y.; Cao, R.; Sanders, J. M.; Song, Y. C.; Zhang, Y. H.; Meints, G. A.; Gao, Y. G.; Mukkamala, D.; Hudock, M. P.; Oldfield, E. *J. Am. Chem. Soc.* **2006**, *128*, 14485−14497.

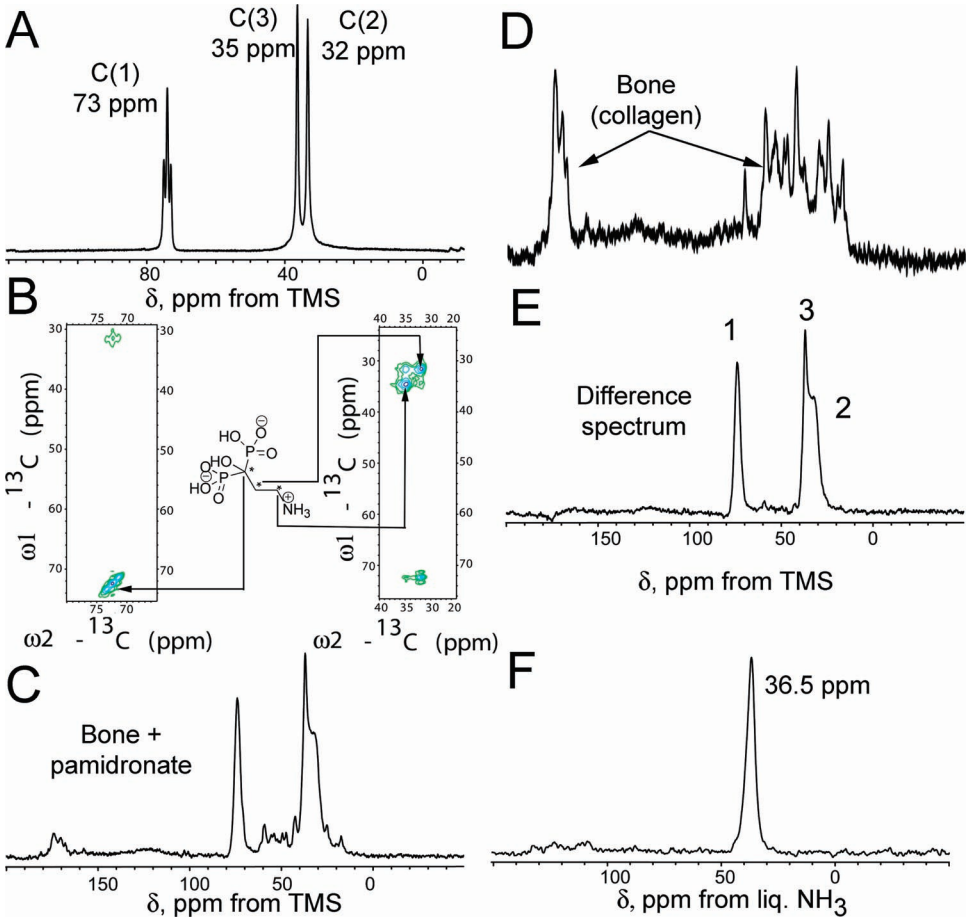

Figure 4. ^{13}C and ^{15}N MAS NMR spectra of [$^{13}C_3$, ^{15}N] pamidronate. (A) ^{13}C NMR spectrum of pamidronate acquired by using a 3 μs ^{1}H 90° pulse width, 2 ms mix time, 50 μs dwell time, 2048 points, 10 s recycle delay, 16 scans, and a 13.333 kHz spin speed. Spectrum was zero-filled to 4096 points and processed with 50 Hz line broadening. (B) $^{13}C-^{13}C$ RFDR correlation spectrum of [$^{13}C_3$, ^{15}N] labeled pamidronate. (C)−(E) ^{13}C NMR spectra of (C) pamidronate on bone; (D) bone; and (E) difference between (C) and (D). All ^{13}C NMR spectra obtained using a 3 μs width 90° pulse, 2 ms mix time, 10 μs dwell time, 2048 points, 10 s recycle delay, 2048 scans and a 13.333 kHz spin speed. Data zero-filled to 4096 points and processed with 50 Hz line broadening. (F) ^{15}N NMR spectrum of [$^{13}C_3$, ^{15}N]-pamidronate on bone, 4 μs ^{1}H 90° pulse width, 5 ms mix time, 50 μs dwell time, 2048 points, 4 s recycle delay, 20 388 scans, and a 13.333 kHz spin speed. Data zero-filled to 4096 points and processed with 50 Hz line broadening.

the C(2), C(3) peaks to high field.[37] These resonances can be unambiguously assigned from an RFDR spectrum (Figure 4B) with C(2) being the most highly shielded peak. When bound to bone, there is a substantial broadening of each resonance (Figure 4C); plus, there are additional small peaks observed. These arise from the glycine, alanine, proline, and hydroxyproline residues in collagen,[38] as shown in Figure 4D. A difference spectrum ([bone + bisphosphonate]-bone) is shown in Figure 4E, and represents the spectrum of pamidronate alone, when bound to bone. The $^{13}C(3)$ line width is small, but that of C(1) (the bisphosphonate backbone carbon) is larger, and that of C(2) is larger still. For C(1), much of the apparent broadening must arise from J-coupling to ^{31}P (see Figure 3A), but this cannot contribute to the breath of C(2). Rather, it seems that here, there is a chemical shift dispersion due, most likely, to *γ-gauche* interactions with a heterogeneous population of phosphonate OH/O^- groups. As expected, the ^{15}N NMR spectrum contains only a single intense resonance, having a chemical shift of 36.5 ppm (from NH_3), consistent with a fully protonated alkylammonium group (Figure 4F). So, ^{13}C and ^{15}N MAS NMR spectra of pamidronate on bone can be readily obtained, opening up the possibility of determining the structure of this bisphosphonate, on human bone. To do this, we employed the *z*-filtered TEDOR method[19] to determine the distances between C(1) and N, which give, in principle, the backbone conformation.

In crystalline sodium pamidronate,[39] the bisphosphonate side chain adopts a close-to-*trans* C(1)−C(2)−C(3)−N configuration, but on bone, the conformation is unknown and could, in principle, be either a *trans* or a *gauche* configuration (*gauche*$^+$ or *gauche*$^-$), with the *gauche* conformations potentially facilitating electrostatic interactions between the terminal ammonium group in the bisphosphonate with anionic groups on the bone surface, due to its "bent" conformation. It also seemed possible that the side chain might actually be quite dynamic, jumping from one anionic bone surface site to another. To deduce the likely backbone conformation, we used the TEDOR experiment.[19] We first investigated as a reference sample [$^{13}C_3$, ^{15}N]-labeled pamidronate, diluted (9%) into natural abundance pamidronate, and cocrystallized as the sodium salt (sample characterized via powder X-ray diffraction). In Na-pamidronate, the 154° (∼*trans*) side-chain conformation corresponds to a 3.82

(37) Harris, R. K.; Merwin, L. H.; Hagele, G. *Magn. Reson. Chem.* **1989**, *27*, 470−475.
(38) Reichert, D.; Pascui, O.; deAzevedo, E. R.; Bonagamba, T. J.; Arnold, K.; Huster, D. *Magn. Reson. Chem.* **2004**, *42*, 276−284.
(39) Vega, D.; Fernendez, D.; Ellena, J. A. *Acta Crystallogr., Sect. C* **2002**, *58*, M77−M80.

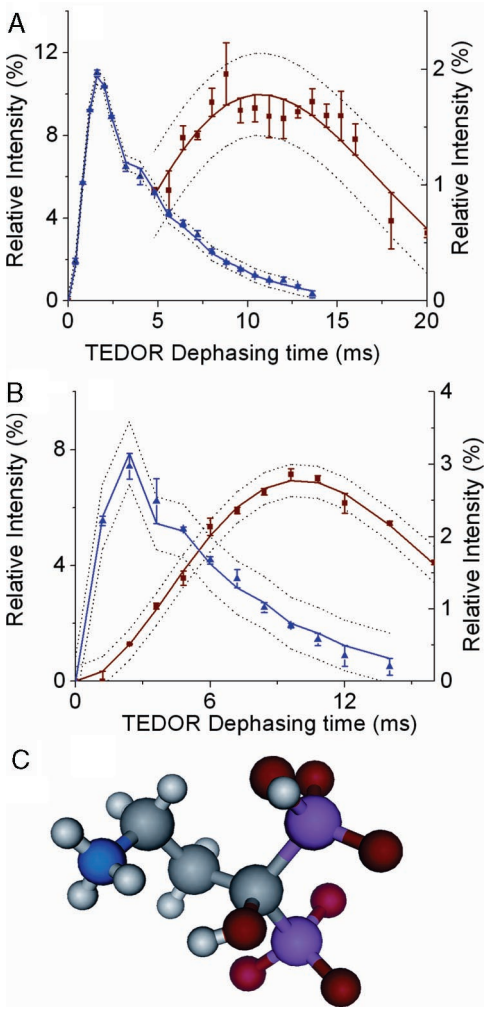

Figure 5. $^{13}C-\{^{15}N\}$ *z*-filtered TEDOR results for (A) [$^{13}C_3$, ^{15}N] labeled pamidronate diluted with 9X natural abundance pamidronate and crystallized as the Na^+ salt; (B) pamidronate on bone at 0 °C. Both samples were spun at 10 kHz, and the recycle time was 2 s. A z-filter period of 200 μs (corresponding to twice the rotor period) with 10 kHz ^1H decoupling was used while an 80 kHz ^1H field was applied for both the CW and TPPM decoupling periods. Peak intensities are normalized to those in a spectrum obtained with a 90° pulse on ^1H, followed by cross polarization to ^{13}C and data acquisition. In (A), the 90° pulse widths were 3 μs for ^1H, 4.5 μs for ^{13}C and 7 μs for ^{15}N. The ^{15}N REDOR 180°-pulse was 14 μs while the ^{13}C refocusing 180° pulse was 9 μs. 8192 scans were used for each point. In (B), the 90° pulse widths were 3.5 μs for ^1H, 5 μs for ^{13}C and 7.5 μs for ^{15}N. The ^{15}N REDOR 180°-pulse was 15 μs, the ^{13}C refocusing 180° pulse was 10 μs. 16 384 scans were used for each point. The experimental results were fit to eqs 8−12 in Jaroniec, et al.[19] by using the Mathematica program. In both (A) and (B), the simulation in blue corresponds to the C(3)−N distance, while red corresponds to the C(1)−N distance, and the dotted lines indicates 95% confidence intervals for the simulation. The typical range of the amplitude scaling factor, λ, was ~0.2−0.5 and the relaxation rate τ was ~70−210 Hz. (C) NMR derived structure of pamidronate on bone. The side chain ($C_1-C_2-C_3-N$) torsion angle is ±71−77°; d = 3.2 Å.

Å C(1)-N distance. The results of a TEDOR experiment on this magnetically dilute sample, Figure 5A, yielded a C(1)−N distance of 3.90 Å, in quite good accord with the crystallographic result (3.82 Å). In contrast, for pamidronate bound to the surface of human bone mineral, the TEDOR result (Figure 5B) yielded a C(1)−N distance, d = 3.2 Å. This is clearly very short and translates to a close to *gauche* backbone conformation ($\chi = \pm 77°$, using the 1.49 Å X-ray C(3)−N bond length; ±71° using the 1.59 Å TEDOR-derived C(3)−N bond length, Figure 5B), shown in Figure 5C. Of course, both *gauche*$^+$ and *gauche*$^-$

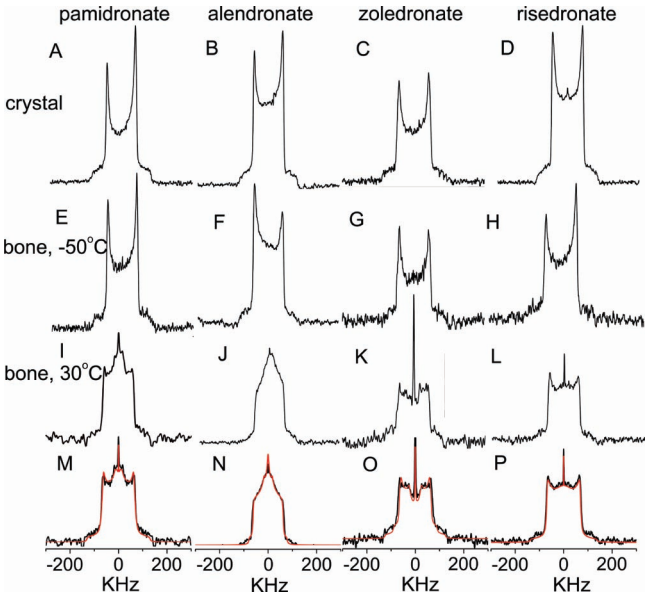

Figure 6. 92 MHz ^2H NMR quadrupole echo NMR spectra of ^2H-labeled bisphosphonates on bone and as crystalline solids. (A−D), bisphosphonates at 30 °C; (A), [$^2H_4$]-pamidronate, (B), [$^2H_6$]-alendronate, (C), [ring-$^2H_3$]-zoledronate, and (D), [ring-$^2H_4$]-risedronate; (E−H), bisphosphonates on bone at −50 °C, in the same order as in (A−D); (I−L), bisphosphonates on bone at 30 °C, in the same order as in (A−D); and, (M−P), deuterium line shape simulations (shown in red) of bisphosphonates bound to bone at 30 °C, in the same order as in (A−D), superimposed on the experimental 30 °C spectra. A small narrow central peak in each case arises from HO^2H. The 90° pulses were typically 2 μs. The interpulse spacing was 40 μs. There was a 25.9 μs delay prior to data acquisition, and FIDs were left shifted to the echo maximum. A 2000 Hz linebroadening was generally applied. The number of scans for bisphosphonates on bone were in the range from 14 810 to 102 819, recycle times were in the range 1−5 s; recycle times for the crystalline bisphosphonates were typically 100 s with ~100 scans being acquired. The kinetic rate (sec^{-1}), conformer ratio, η, QCC (kHz) and jump angles (degrees) were as follows: pamidronate, 3×10^7, 1:1, 0.05, 175, ±65; alendronate, 5×10^6, 1:1, 0.05, 167, ±60 (for both the side-chain torsion angles); zoledronate, 5×10^6, 1:1, 0.068, 185, ±35; risedronate, 3×10^6, 1:4, 0.05, 185, ±60; A 50% attenuation of the C^β, C^δ CH_2 groups in alendronate was used to reflect their larger T_1 values. In the case of zoledronate, the intensity used for $^2H(5)$ was only 20%, due to $^2H/^1H$ exchange during synthesis (based on 500 MHz solution ^1H NMR).

conformers would be consistent with the NMR results and because the two forms are mirror images, neither would be preferred (and indeed, as discussed below, it appears that the two forms interconvert, via 2-site jumps). In any case, the TEDOR results strongly suggest that the pamidronate side chain maximizes its electrostatic interaction with the bone mineral surface (carbonatoapatite and hydroxyapatite) via NH_3^+ (pamidronate)-PO_4^{3-} (or CO_3^{2-}) (bone mineral) interactions. That is, the bisphosphonate side chain is "bent" over, in order to enhance this interaction.

Of course, the interactions of the bisphosphonate side chains with bone could be quite dynamic, even though the bisphosphonate backbones are not highly mobile. To investigate this possibility, we determined the ^2H NMR spectra of side chain ^2H-labeled pamidronate, alendronate, zoledronate, and risedronate, bound to bone. Reference ^2H NMR spectra for each of the pure bisphosphonates at 30 °C are shown in Figure 6A−D, with each clearly indicating the absence of any significant side chain mobility at 30 °C, on the $\sim 10^{-5}$ s time scale of the ^2H NMR experiment. Essentially the same spectra are observed for each bisphosphonate when bound to bone, at −50 °C (Figure

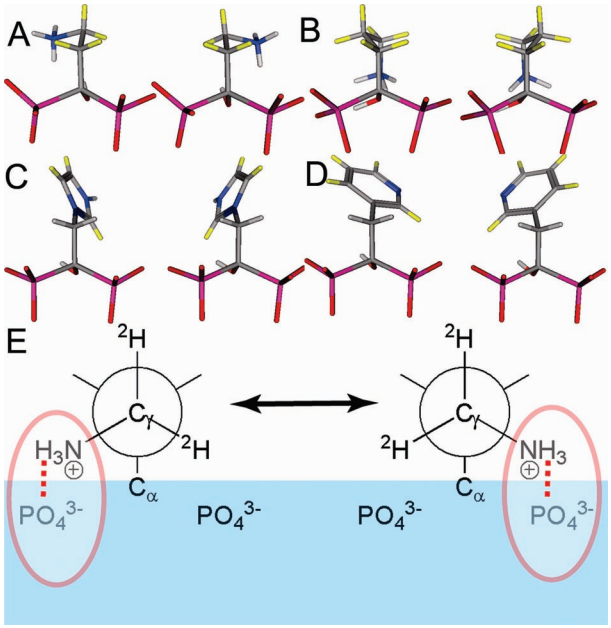

Figure 7. Models for bisphosphonates on bone depicting proposed side-chain motions: nitrogen = cyan; deuterium = yellow; carbon = gray; oxygen = red; phosphorus = pink. (A), pamidronate *gauche*$^+$/*gauche*$^-$ side-chain motion leading to a backbone torsional oscillation of ~±65°; (B), alendronate undergoing tetrahedral or "mirror image" jump motion; (C), zoledronate undergoing ±30° ring wobbles and, (D), risedronate undergoing ±60° ring wobbles. With the exception of risedronate, all the side chains are shown protonated. (E), Schematic of pamidronate on bone depicting motional averaging model for $^2H^\gamma$.

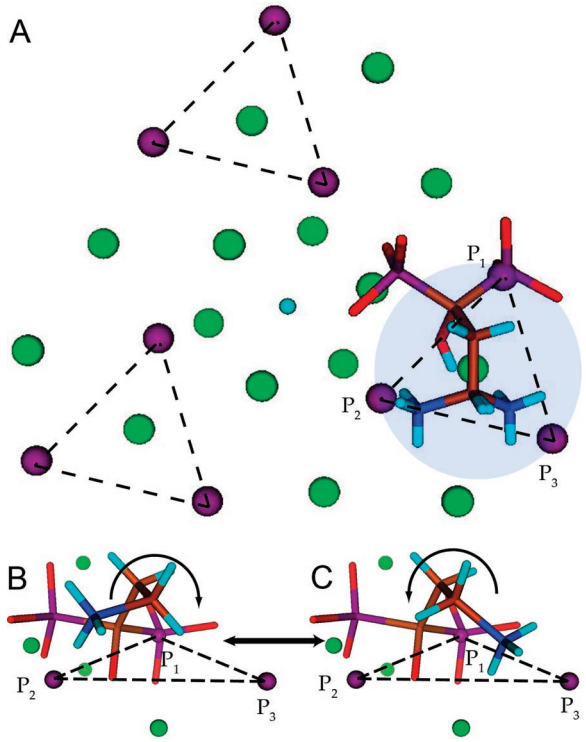

Figure 8. Molecular models for pamidronate-bone (HAP) interactions. (A), Top view of pamidronate bound in *gauche*$^+$/*gauche*$^-$ conformations to a PO_4^{3-} in one of the three ^{31}P-triangles in the unit cell of HAP. (B, C), two views of pamidronate (carbon in brown; oxygen in red and hydrogen in cyan) side chain NH_3^+ (dark blue) binding to one or other of the PO_4^{3-} (P = purple) groups (P_2 or P_3) in the "P_3-triangle", the bisphosphonate PO_3 group occupies the third site (P_1). The 1-OH group interacts with a Ca^{2+} (green) below. The $^{13}C^\gamma$—$^{31}PO_4^{3-}$ distance is much shorter than the $^{13}C^\beta$—PO_4^{3-} and $^{13}C^\alpha$—$^{31}PO_4^{3-}$ distances and the two conformations and interactions shown are consistent with the TEDOR, ^{2}H and DCP NMR results.

6E−H). However, at 30 °C, there are clearly spectral line shape changes (Figure 6I−L), indicating the presence of side chain mobility. We thus next performed ^{2}H NMR line shape simulations for all four ^{2}H-labeled bisphosphonates on bone (at 30 °C), as shown in Figure 6M−P, in which the line shape simulations (in red) are superimposed on the experimental spectra (in black). The models used are shown in Figure 7A−D. In the case of pamidronate, the results of the TEDOR experiments indicated the likely existence of a *gauche* conformation, with a C(1)-N torsion angle of ~±71−77° (~*gauche*$^+$, ~*gauche*$^-$). As *gauche*$^+$ and *gauche*$^-$ are equally energetically likely, this suggested a simple two-site model (Figure 7A) in which *gauche*$^+$ and *gauche*$^-$ forms interconvert, and the results of a ^{2}H-line shape simulation in which the $-CH_2-NH_3^+$ group undergoes a 2-fold hop (±65°) between *gauche*$^+$ and *gauche*$^-$ at ~3 × 10^7 s^{-1}, due perhaps to the $-CH_2-NH_3^+$ group sampling two different anionic binding sites, was found to be in good agreement with experiment (Figure 6M). In the case of alendronate, the line shape is very different from that seen with pamidronate, and closely resembles that seen previously in ^{2}H NMR spectra of ^{2}H-labeled gel-state lipids,[40] where the CH_2 groups undergo fast but restricted two-site hopping. One possible motion for the alendronate side chain, shown in Figure 7B, would be a "mirror-image" jump in which all three CH_2 groups undergo motional averaging. In this case, the NH_3^+ group remains in the same location, but there are coupled rotations at each site in the side chain and again, the results of a line shape simulation are in good agreement with experiment, Figure 6N. For zoledronate, we find good accord (Figure 6O) for a ±30° ring wobble (Figure 7C) and for risedronate, there is again evidence for restricted motion that freezes out at low temperatures (Figure 6H), with the results of a line shape simulation (Figure 6P) suggesting a ±60° ring wobble with a 1:4 conformer population, at 30 °C. While further work with, for example, specifically ^{2}H-labeled bisphosphonates, will be needed in order to obtain more detailed motional models, what is clear from the results of Figures 6 and 7 is that the side chains of each bisphosphonate undergo fast (but restricted) motions when bound to bone. In contrast, none of the crystalline bisphosphonates undergo fast side-chain motion, and all of the side chain motions on bone are frozen out at −50 °C. In the case of pamidronate, fast *gauche*$^+$/*gauche*$^-$ isomerization is indicated (at 30 °C) from the ^{2}H NMR line shape simulation and is consistent with the TEDOR result (at 0 °C), which also indicates the presence of a gauche conformer. In this case, only the C-3 or γ-protons are affected, as illustrated in Figure 7E. For alendronate, the line shape is similar to that seen previously in gel state lipids, and suggests restricted tetrahedral jumps (e.g., between the "mirror-images" shown in Figure 7B). For zoledronate and risedronate, the situation is more complex, since both protonated and neutral rings could be present. However, there is clearly no evidence for rapid 180° ring flips in either zoledronate or risedronate, since these would be expected to result in $\eta \approx 0.65$ line shapes, as observed, e.g., for phenylalanine residues in proteins and in zwitterionic phenylalanine.[41] This can of course be attributed to the presence of the basic

(40) Huang, T. H.; Skarjune, R. P.; Wittebort, R. J.; Griffin, R. G.; Oldfield, E. *J. Am. Chem. Soc.* **1980**, *102*, 7377−7379.

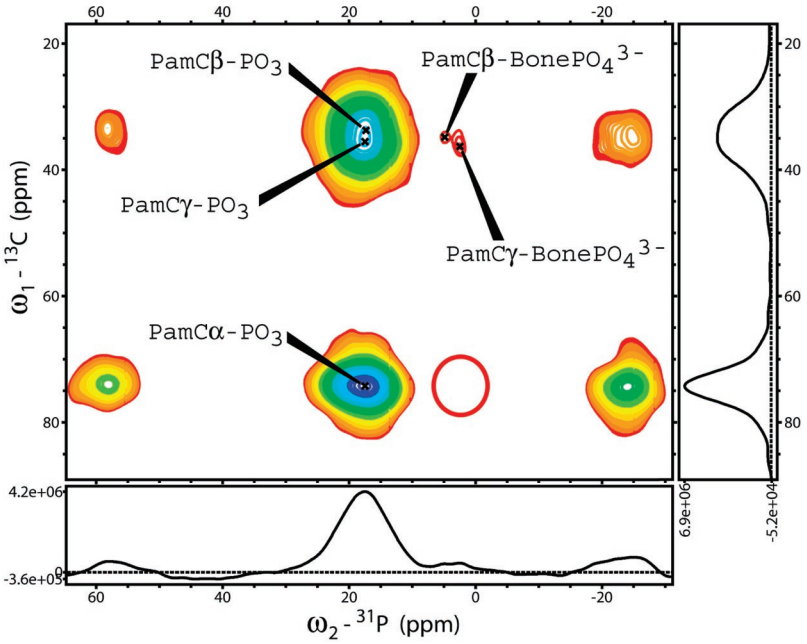

Figure 9. Double cross-polarization spectrum ($^1H \rightarrow {}^{13}C \rightarrow {}^{31}P$) of [$^{13}C_3$, ^{15}N] pamidronate on human bone. The experiment was performed at a spinning speed of 10 kHz with a ^1H 90° pulse width of 3.5 μs, a $^1H \rightarrow {}^{13}C$ mix time of 0.8 ms followed by t_1 evolution, a $^{13}C \rightarrow {}^{31}P$ mix time of 6 ms followed by data acquisition using 2048 points and a dwell time of 10 μs. Power levels for the $^{13}C \rightarrow {}^{31}P$ transfer were matched to $\omega_C = (5/2)\omega_R$ and $\omega_P = (7/2)\omega_R$ in order to facilitate a broadband transfer covering all the peaks of interest in both dimensions. The indirect dimension was sampled with 64 real points (TPPI[44]) with a dwell time of 20 μs and 2048 scans were acquired per row with a recycle delay of 2 s. TPPM decoupling of ~80 kHz (6 μs and 16° phase shifted) was used during chemical shift evolution and acquisition periods while ~75 kHz CW decoupling was used during the $^{13}C \rightarrow {}^{31}P$ transfer. Two such experiments with a total acquisition time of ~6 days were added before processing. The cross-peak volume for $^{13}C^{\gamma}-{}^{31}PO_4^{3-}$ is large and indicates close proximity between $^{13}C^{\gamma}$ and bone $^{31}PO_4^{3-}$ groups. There are only small or no significant cross-peak volumes for $^{13}C^{\beta}$, $^{13}C^{\alpha}$ and $^{31}PO_4^{3-}$, due to longer (3.75, 3.90 Å) $^{13}C-{}^{31}P$ distances as compared to $^{13}C^{\gamma}-{}^{31}PO_4^{3-}$ (3.03 Å, on average, from the models shown in Figure 8).

nitrogen atoms in both bisphosphonates, which can interact electrostatically or via hydrogen bonds, with bone surface groups.

3.3. Molecular Model for Pamidronate on Bone. Finally, we propose a detailed molecular model for pamidronate binding to the mineral component of human bone at pH = 7 at 300 K. As can be seen from the results presented above, there are numerous pieces of the puzzle that need to be assembled. Pamidronate binds in a chemisorption process, releasing ~1 inorganic phosphate per bisphosphonate bound, and this process follows a classical first-order Langmuir isotherm, from which we deduce a surface area per pamidronate of ~30−38 Å^2 at θ=1. The results of the TEDOR experiment indicate that the pamidronate side chain adopts a *gauche* as opposed to a *trans* conformation (at 0 °C), whereas the ^2H NMR results indicate that at 30 °C there is (±65°) hopping between 2 states and that this process is frozen out at −50 °C. The simplest explanation for these observations would of course be that the side chain conformational change is *gauche*$^+$ ↔ *gauche*$^-$, and we see from Figure 7E that this "hop" affects (or motionally averages) just the C$^{\gamma}$ protons.

Next, we need to see how the bisphosphonate PO_3 group might bind to bone mineral. To do this, we inspected the X-ray crystallographic structure of hydroxyapatite.[42] The structure is characterized by several relatively close-packed triangular arrangements of PO_4^{3-} groups, and we propose that one of the two phosphonate groups in a bisphosphonate (P atoms are shown in purple in Figure 8A) displaces one bone mineral PO_4^{3-}(*P*1), as shown in Figure 8B,C. This packing arrangement gives an immediate explanation for the presence of a gauche side chain configuration, because in this conformation, the terminal $^+NH_3$ group can interact electrostatically with either one of the two remaining PO_4^{3-} groups (P_2/P_3) in the "P_3-triangle", as shown in Figure 8B,C. The conformations of the side chains are either *gauche*$^+$ or *gauche*$^-$, and based on the ^2H NMR results, we propose that these conformations can rapidly interconvert, at 30 °C. The model also reveals that the 1-OH group is adjacent to a Ca^{2+}, explaining the importance of this group for bone binding since a sizable ion-dipole interaction would be expected. To try to further test this model, we carried out a double cross polarization experiment ($^1H \rightarrow {}^{13}C \rightarrow {}^{31}P$) on [$^{13}C_3$, ^{15}N] pamidronate on bone: the result is shown in Figure 9. As can be seen in the Figure, there is a major cross-peak between the $^{13}C^{\gamma}$ and $^{31}PO_4^{3-}$ bone mineral peaks, a smaller cross-peak between $^{13}C^{\beta}$ and $^{31}PO_4^{3-}$, but no observable cross-peak between $^{13}C^{\alpha}$ and bone mineral. The $^{13}C^{\gamma}-{}^{31}P$ cross-peak volume is by far the largest and is consistent with the short (average) $^{13}C^{\alpha}-{}^{31}PO_4^{3-}$ distance of ~3.03 Å found from the model (Figure 8), whereas the $^{13}C^{\beta}$ and $^{13}C^{\alpha}-{}^{31}PO_4^{3-}$ distances are clearly much longer, ~3.75 and 3.9 Å, respectively. These results therefore strongly support a "bent-over" side chain conformation in which the $^+NH_3$ group interacts with the bone surface, consistent with the TEDOR and ^2H NMR results which indicate *gauche*$^+$/*gauche*$^-$ side-chain conformations.

4. Conclusions

In summary, the results discussed above can be viewed together to provide the first detailed spectroscopic picture of how bisphosphonates bind to human bone. First, and independent of any molecular model of binding, bisphosphonate

(41) Kinsey, R. A.; Kintanar, A.; Oldfield, E. *J. Biol. Chem.* **1981**, *256*, 9028−9036.
(42) Wilson, R. M.; Elliott, J. C.; Dowker, S. E. P. *Am. Mineral.* **1999**, *84*, 1406−1414.

backbones bind to bone in a "rigid" or irrotational manner, at least on the time scale of the inverse of the ^{31}P chemical shielding tensor anisotropy ($\sim\mu$s). That is, the overall breadths of the ^{31}P shielding tensors in crystalline bisphosphonates are very similar to those found for bisphosphonates on bone, and there is no evidence for fast surface diffusion, which would be expected to average the CSA. Second, we find that inorganic phosphate is released when bisphosphonates bind to bone, indicating a displacement mechanism in which the bisphosphonates are "chemically" bonded to the bone matrix. This would be consistent with the observation that high levels of P_i are needed for the chromatographic elution of bisphosphonates from HAP. Third, we find that pamidronate binding can be well described by a Langmuir adsorption isotherm, that the surface area/pamidronate is $\sim$30−38 Å^2 and that ΔG for binding is $\sim$−4.3 kcal mol^{-1} (at pH = 7, 30 °C). Fourth, the results of ^{15}N NMR measurements indicate that zoledronate binds in a "partially" protonated form at pH 7, risedronate is non-protonated, while pamidronate is essentially fully protonated, consistent with known pK_a values for imidazole (p$K_a \approx 6.7$), pyridine (p$K_a \approx 5.7$) and primary amines (p$K_a \approx 10.5$). Fifth, the results of TEDOR experiments show that pamidronate binds in a close-to-*gauche* conformation, which suggests that the terminal ammonium group might bind in such a way as to maximize its electrostatic interactions with anionic groups in the bone mineral. Sixth, the results of ^2H NMR measurements indicate that pamidronate undergoes fast conformational changes (3×10^7 sec^{-1}) on bone, interconverting most likely between *gauche*$^+$ and *gauche*$^-$ conformers. In contrast, alendronate undergoes a series of coupled rotations, yielding lineshapes and linewidths very similar to those seen previously with ^2H-labeled lipids.[40] With the aromatic bisphosphonates, there are rapid ($\sim 3 - 5 \times 10^7$ sec^{-1}) ring "wobbles", although we find no evidence for the $\eta \approx 0.65$ lineshapes seen with aromatic groups (i.e., phenylalanine) in proteins, in which 2-fold 180° ring-flips occur. Seventh, the results of a double cross-polarization experiment indicate that the pamidronate side chain C^γ carbon is close to bone mineral PO_4^{3-} groups, while C^α and C^β carbons are more distant. Overall, these results enable the construction of a molecular model for pamidronate binding to bone in which the chemisorbed bisphosphonate displaces one bone PO_4^{3-} in the hydroxyapatite (carbonatoapatite) triangle of PO_4^{3-} groups, enabling the *gauche* conformers (from TEDOR) to interconvert (from ^2H NMR), jumping from one PO_4^{3-} site to another (from DCP).

Given that bisphosphonates represent a large contribution to the global pharmaceutical market and that there is interest in their further development for use in oncology and as anti-infectives, the results presented above are of general interest in the context of tailoring new bisphosphonates to suit their intended application. In particular, the ability to begin to probe both the binding affinities (ΔG, and in principle of course ΔH and ΔS) as well as the static structures of bisphosphonates bound to human bone should help with the development of novel species that have particular attributes by using, for example, the types of structure-based design techniques used to develop enzyme inhibitors. For example, it has recently been shown that bisphosphonate activity in bone resorption *in vivo* can be well described by using a simple statistical model involving enzyme (FPPS) and HAP affinity data:[43] an obvious extension of this would be to use enzyme QSAR and structure-based bone binding results. In addition, it should also be possible to further develop the static (and dynamic) models described above, to help validate computational modes for bone (HAP)-bisphosphonate interactions.[10]

Acknowledgment. This work was supported by the United States Public Health Service (NIH Grant No. GM65307). S.M. was supported by an American Heart Association, Midwest Affiliate, Predoctoral Fellowship (Award Number 0615564Z). Y.S. was supported by a Leukemia and Lymphoma Society Special Fellowship (Award No. 3019-06). The authors would like to thank Professor Robert Griffin and Dr. Patrick van der Wel for providing the Turbopowder program, Professor Chad Rienstra, for helpful advice, and Dushyant Mukkamala, for help with the X-ray measurements.

JA0759949

(43) Ebetino, F. H.; B. L. B.; Evdokimov, A. G.; Pokross, M.; Kavanagh, K.; Lundy, M.; McKenna, C. E.; Russell, R. G. G.; Dao, Z.; Dunford, J. *Abstract 136, CERMACS ACS Regional Meeting,* (Cincinatti, Ohio) **2007**.
(44) Marion, D.; Wuthrich, K. *Biochem. Biophys. Res. Commun.* **1983**, *113*, 967−974.